Int. J. Solids Structures Vol. 23, No. 10, pp. 1373–1385, 1987
Printed in Great Britain.

0020-7683/87 $3.00+ .00

THE SLIDING INCLUSION UNDER SHEAR

I. JASIUK,† E. TSUCHIDA‡ and T. MURA
Department of Civil Engineering, Northwestern University, Evanston, IL 60201, U.S.A.

(*Received* 6 *August* 1986; *in revised form* 10 *February* 1987)

Abstract—The elastic fields due to a spheroidal inclusion, which undergoes constant shear eigenstrains and a spheroidal inhomogeneity under uniform shear stress applied at infinity are investigated. The interface between the material and the spheroid allows free sliding (cannot sustain shear tractions). The Papkovich–Neuber displacement potentials in the form of infinite series are used in the analysis. The dependence of stresses and displacements on the shear moduli ratio, Poisson's ratio and the shape of the subdomain is analyzed. It is discovered that stresses in the sliding spheroidal subdomain are not uniform, unlike the perfectly bonded inclusion solution where Eshelby's result holds. The applications to the evaluation of average elastic properties of the composites with sliding interfaces are also investigated and it is observed that sliding causes relaxation of the elastic moduli.

INTRODUCTION

Eshelby[1] discovered that when an ellipsoidal inclusion undergoes a transformation strain or an ellipsoidal inhomogeneity disturbs a field of applied stresses, the stresses are uniform inside the ellipsoidal domain. A similar result has been obtained by Edwards[2] for the spheroidal subdomain. In both cases, the perfect bond was assumed at the interface, which implies continuity of tractions and displacements.

This paper investigates the other important model which allows free sliding on the ellipsoidal interface. It assumes the continuity of tractions and normal displacements and also the vanishing shear tractions along the interface S, i.e.

$$[\sigma_{ij}]n_j = 0 \qquad \text{on } S \tag{1}$$

$$[u_i]n_i = 0 \qquad \text{on } S \tag{2}$$

and

$$\sigma_{ij}n_j - \sigma_{jk}n_j n_k n_i = 0 \qquad \text{on } S \tag{3}$$

where [ ] = (out) − (in) and n_i is the normal vector on S. Physically, this model may represent grain boundary sliding in polycrystals, behavior of precipitates at high temperatures or imperfectly bonded interfaces in composite materials.

The spheroidal inhomogeneity or inclusion considered in this paper is embedded in an elastic material and is subjected to a constant pure shear loading at infinity or undergoes a constant shear eigenstrain (transformation strain, thermal expansion, initial or plastic strain, etc.). This analysis supplements the three-dimensional sliding inclusion solutions obtained by Ghahremani[3], Mura and Furuhashi[4], Wong and Barnett[5] and Mura *et al.*[6].

Mura and Furuhashi[4] solved a similar problem when the ellipsoidal inclusion is subjected to constant shear eigenstrains and discovered the surprising result that the stress field vanishes everywhere. Their solution, however, is restricted to the ellipsoidal shape such that $a_i \neq a_j$, where a_j are the semi-axes of the ellipsoid.

This paper investigates the case when the inclusion is of prolate or oblate spheroidal shape (ranging from a cylinder or needle to a disk) such that $a_1 = a_2 \neq a_3$. For this geometry,

† Present address: Department of Metallurgy, Mechanics and Materials Science, Michigan State University, East Lansing, MI 48824-1226, U.S.A.
‡ Faculty of Engineering, Saitama University, 255 Shimo-Okubo, Urawa, Japan.

the stress field is not zero anymore, and due to sliding it is not uniform as in Eshelby's inclusion. The solution presented here is expressed in terms of Papkovich–Neuber displacement potentials in the form of infinite series. The method of solution is similar to the one of the axisymmetric problem[6] and will be discussed on the example of prolate spheroidal shape. The solution for the oblate spheroidal inclusion is obtained in an analogous way by using the oblate spheroidal coordinate system.

METHOD OF SOLUTION

Consider an infinite, elastic, homogeneous and isotropic material having a prolate spheroidal subdomain as shown in Fig. 1. The problem is to determine the stress and displacement field when the inhomogeneity is under shear loading at infinity or when the inclusion undergoes a constant shear eigenstrain. Sliding is allowed at the interface and shear tractions are specified to vanish but no debonding takes place.

Let the origin of coordinates "0" be at the center of the spheroid and the coordinate axes be coincident with the spheroid's axes of symmetry. The z-axis is chosen to be in the major axis direction. The prolate spheroidal coordinate system (α, β, γ) is related to Cartesian coordinates (x, y, z) by the transformation equations

$$\begin{aligned} x &= c \sinh \alpha \sin \beta \cos \gamma \\ y &= c \sinh \alpha \sin \beta \sin \gamma \\ z &= c \cosh \alpha \cos \beta \end{aligned} \tag{4}$$

where c is a positive constant (half-distance between foci) and

$$0 \leqslant \alpha < \infty, \qquad 0 \leqslant \beta \leqslant \pi, \qquad 0 \leqslant \gamma \leqslant 2\pi. \tag{5}$$

The surfaces $\alpha = \text{const}$, $\beta = \text{const}$ and $\gamma = \text{const}$ form an orthogonal family of prolate spheroids, hyperboloids of two sheets and half planes passing through the z-axis.

The surface of the ellipsoid is defined by $\alpha = \alpha_0$ and the minor and major semi-axes are $a = c \sinh \alpha_0$ and $b = c \cosh \alpha_0$. The differential arc length ds is in the form

$$(ds)^2 = (d\alpha/h_1)^2 + (d\beta/h_2)^2 + (d\gamma/h_3)^2 \tag{6}$$

where metric coefficients h_i are

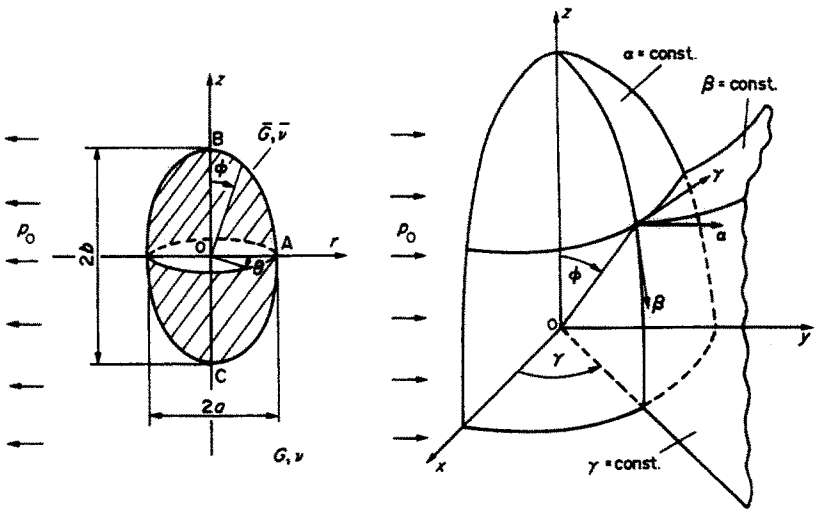

Fig. 1. Spheroidal coordinate system.

$$h_1 = h_2 = 1/[c(\cosh^2 \alpha - \cos^2 \beta)], \qquad h_3 = 1/(c \sinh \alpha \sin \beta). \tag{7}$$

For convenience we introduce new variables

$$\begin{aligned} q &= \cosh \alpha, \qquad \bar{q} = \sinh \alpha \\ p &= \cos \beta, \qquad \bar{p} = \sin \beta \end{aligned} \tag{8}$$

such that $1 \leqslant q < \infty$ and $-1 \leqslant p \leqslant 1$ (from eqn (5)).

The Papkovich–Neuber potentials ϕ_0 and $\underset{\sim}{\phi}$ are used in the analysis. The general solution of the Navier elastostatic equation in the absence of body forces can be expressed in terms of four scalar harmonic functions: ϕ_0 and three Cartesian components ϕ_1, ϕ_2 and ϕ_3 of $\underset{\sim}{\phi}$ such that

$$2G[u_x, u_y, u_z] = \text{grad } (\phi_0 + x\phi_1 + y\phi_2 + z\phi_3) - 4(1-\nu)[\phi_1, \phi_2, \phi_3] \tag{9}$$

where G and ν are the shear modulus and Poisson's ratio, respectively. When the equation refers to the inhomogeneity, G and ν are taken as $\bar{G}$ and $\bar{\nu}$.

The displacements expressed by eqn (9) are transformed to the prolate coordinate system and are related to strains as shown by Love[7].

The sliding boundary conditions (1)–(3) at the interface $\alpha = \alpha_0$ are

$$\begin{aligned} &(u_\alpha)_{\alpha=\alpha_0} = (\bar{u}_\alpha)_{\alpha=\alpha_0}, && (\sigma_\alpha)_{\alpha=\alpha_0} = (\bar{\sigma}_\alpha)_{\alpha=\alpha_0} \\ &(\tau_{\alpha\beta})_{\alpha=\alpha_0} = 0, && (\bar{\tau}_{\alpha\beta})_{\alpha=\alpha_0} = 0 \\ &(\tau_{\alpha\gamma})_{\alpha=\alpha_0} = 0, && (\bar{\tau}_{\alpha\gamma})_{\alpha=\alpha_0} = 0. \end{aligned} \tag{10}$$

The quantities referring to inclusion are denoted by a bar.

The stress state at infinity when shear loading is applied is

$$\begin{aligned} (\sigma_x)_{r\to\infty} &= -(\sigma_y)_{r\to\infty} = p_0 \\ (\sigma_z, \tau_{xz}, \tau_{yz})_{r\to\infty} &= 0. \end{aligned} \tag{11}$$

When the inclusion is under eigenstrain loading, the stresses vanish at infinity.

The eigenstrains are $\varepsilon_x^* = -\varepsilon_y^* \neq 0$. The displacements inside the inclusion are the sum of free deformation

$$\bar{u}_x^* = \varepsilon_x^* x, \qquad \bar{u}_y^* = -\varepsilon_x^* y \tag{12}$$

and the displacements obtained from eqn (9).

After transforming stresses and displacements obtained from eqn (9) into the prolate spheroidal coordinate system, stress and displacement fields are determined by choosing the proper harmonic potential functions ϕ_0, ϕ_1, ϕ_2, ϕ_3.

The general form of potentials in the prolate coordinate system as stated by Hobson[8] is:

for the space interior to a prescribed spheroid $\alpha = \alpha_0$ (inclusion)

$$P_n^m(q) P_n^m(p) \begin{matrix}\cos \\ \sin\end{matrix} m\gamma; \tag{13}$$

and for the space exterior to α_0 (matrix)

$$Q_n^m(q)P_n^m(p)\begin{matrix}\cos\\ \sin\end{matrix} m\gamma. \tag{14}$$

The suitable displacement potentials for the discussed boundary value problem are chosen as follows:

for the matrix region ($\alpha > \alpha_0$)

$$\begin{aligned}
&[\mathrm{I}] \quad \phi_0 = C_0 \sum_{n=2}^{\infty} A_n Q_n^2(q) P_n^2(p) \cos 2\gamma \\
&[\mathrm{II}] \quad \begin{cases} \phi_1 = C_0 \sum_{n=1}^{\infty} B_n Q_n^1(q) P_n^1(p) \cos \gamma \\ \phi_2 = -C_0 \sum_{n=1}^{\infty} B_n Q_n^1(q) P_n^1(p) \sin \gamma \end{cases} \\
&[\mathrm{III}] \quad \phi_3 = C_0 \sum_{n=2}^{\infty} C_n Q_n^2(q) P_n^2(p) \cos 2\gamma;
\end{aligned} \tag{15}$$

and for the inclusion region ($\alpha < \alpha_0$)

$$\begin{aligned}
&[\mathrm{IV}] \quad \phi_0 = C_0 \sum_{n=2}^{\infty} \bar{A}_n P_n^2(q) P_n^2(p) \cos 2\gamma \\
&[\mathrm{V}] \quad \begin{cases} \phi_1 = C_0 \sum_{n=1}^{\infty} \bar{B}_n P_n^1(q) P_n^1(p) \cos \gamma \\ \phi_2 = -C_0 \sum_{n=1}^{\infty} \bar{B}_n P_n^1(q) P_n^1(p) \sin \gamma \end{cases} \\
&[\mathrm{VI}] \quad \phi_3 = C_0 \sum_{n=2}^{\infty} \bar{C}_n P_n^2(q) P_n^2(p) \cos 2\gamma
\end{aligned} \tag{16}$$

where

$$C_0 = \begin{cases} p_0 & \text{for loading at infinity} \\ 2G\varepsilon_x^* & \text{for eigenstrain case.} \end{cases}$$

$P_n^m(p)$ and $Q_n^m(q)$ ($m = 1, 2$) are associated Legendre's functions of the first and second kind of order $m = 1$ or 2 and

$$\begin{aligned}
P_n^m(x) &= |x^2-1|^{m/2} \frac{\mathrm{d}^m}{\mathrm{d}x^m} P_n(x) \\
Q_n^m(x) &= (x^2-1)^{m/2} \frac{\mathrm{d}^m}{\mathrm{d}x^m} Q_n(x)
\end{aligned} \tag{17}$$

where

$$P_n(x) = \frac{1}{2^n n!} \frac{\mathrm{d}^n}{\mathrm{d}x^n} (x^2-1)^n$$

$$Q_n(x) = \frac{1}{2} P_n(x) \log \frac{1+x}{1-x} - W_{n-1}(x)$$

$$W_{n-1}(x) = \sum_{r=1}^{n} \frac{1}{r} P_{r-1}(x) P_{n-r}(x).$$

The stresses and displacements obtained from potentials in eqn (15) vanish at infinity.

The undisturbed stress and displacement fields (before the introduction of inhomogeneity) due to the shear loading $\sigma_x^0 = -\sigma_y^0 = p_0$ applied at infinity are transformed into the prolate spheroidal coordinate system. The undisturbed displacement field u_α^0 and stresses σ_α^0, $\tau_{\alpha\beta}^0$ and $\tau_{\alpha\gamma}^0$ needed for continuity equations, eqns (10), expressed in terms of associated Legendre's functions $P_n^2(p)$ are

$$\begin{aligned}
\frac{2Gu_\alpha^0}{p_0 \cos 2\gamma} &= c^2 h q \bar{q} p^2 = h\bar{q}\left\{c^2 q \frac{P_2^2(p)}{3}\right\} \\
\frac{\sigma_\alpha^0}{p_0 \cos 2\gamma} &= q^2 - c^2 h^2 q^2 \bar{q}^2 = c^2 h^4 \left\{c^2 q^2 \left[\left(\frac{\bar{q}^2}{3} + \frac{2}{7}\right) P_2^2(p) - \frac{2}{105} P_4^2(p)\right]\right\} \\
\frac{\tau_{\alpha\beta}^0}{p_0 \cos 2\gamma} &= c^2 h^2 q \bar{q} p \bar{p} = c^2 h^4 \overline{qp}\left\{-c^2 \frac{q\bar{q}^2}{6} P_2^{2'}(p) + c^2 \frac{q}{15} P_3^2(p)\right\} \\
\frac{\tau_{\alpha\gamma}^0}{p_0 \sin 2\gamma} &= -chq\bar{p} = \frac{2h}{c\bar{q}^2 \bar{p}}\left[-\frac{c^2}{2} q\bar{q}^2 \bar{p}^2\right] = \frac{2h}{c\bar{q}^2\bar{p}}\left\{-c^2 \frac{q\bar{q}^2}{6} P_2^2(p)\right\}
\end{aligned} \tag{18}$$

where $P_n^{2'}(p)$ is the derivative of $P_n^2(p)$.

Similarly, the free deformation in the inclusion due to the constant shear eigenstrain $\varepsilon_x^* = -\varepsilon_y^*$ is

$$\frac{2G\bar{u}_\alpha^*}{(2G\varepsilon_x^*)\cos 2\gamma} = c^2 h q \overline{qp}^2 = h\bar{q}\left\{c^2 q \frac{P_2^2(p)}{3}\right\}. \tag{19}$$

The stresses and displacements, eqns (18) and (19), due to the applied load are combined with the stresses and displacements due to the inclusion or inhomogeneity disturbance derived from potentials (15) and (16). Since the expressions obtained from eqns (15) vanish at infinity, the boundary conditions at infinity are satisfied.

In order to satisfy the sliding boundary conditions, eqns (10), we substitute these combined stresses and displacements into eqns (10) and after the use of recursion formulas for the Legendre functions, we equate coefficients of $P_n^2(p)$ and $P_n^{2'}(p)$. This way we obtain an infinite system of algebraic equations for the unknown constants A_n, B_n, C_n, $\bar{A}_n$, $\bar{B}_n$ and $\bar{C}_n$. In the numerical calculations the infinite series are truncated at $n = N$ and the truncation number is chosen so the stresses and displacement in the continuity equations match to three significant figures. It is found that A_n and $\bar{A}_n$ ($n = 3, 5, \ldots$), B_n and $\bar{B}_n$ ($n = 2, 4, \ldots$) and C_n and $\bar{C}_n$ ($n = 2, 4, \ldots$) are zero, because the stresses are symmetrical about the x–y plane.

After evaluating the constants A_n, B_n, C_n, $\bar{A}_n$, $\bar{B}_n$ and $\bar{C}_n$, we can represent the stress and displacement fields everywhere in the inclusion and in the matrix.

AVERAGE SHEAR MODULI

The results obtained for an isolated inhomogeneity are used directly for an estimation of the macroscopic elastic properties of the composite. The parameters considered are the moduli ratio, shape and interface effect (sliding). Since the pure shear loading $\sigma_x^0 = -\sigma_y^0 = p_0$ is applied, we will estimate the average shear modulus in the x–y plane.

When an isolated sliding inhomogeneity Ω in domain D is subjected to an applied stress σ_{ij}^0 at infinity, the elastic strain energy is expressed as

$$W^* = \frac{1}{2}\int_D (\sigma_{ij}^0+\sigma_{ij})(u_{i,j}^0+u_{i,j})\,dV \tag{20}$$

where u_i^0 is the displacement due to the applied load in the absence of inhomogeneity and σ_{ij} and u_i are the stress and displacement disturbances due to the presence of inhomogeneity and sliding. σ_{ij} satisfies the equations of equilibrium $\sigma_{ij,j}=0$ in D and the traction free condition $\sigma_{ij}n_j=0$ on $|D|$, the boundary of D. The stress–strain relations are

$$\begin{aligned} \sigma_{ij}^0 &= C_{ijkl}\varepsilon_{kl}^0 && \text{in } D \\ \sigma_{ij}^0+\sigma_{ij} &= C_{ijkl}(u_{k,l}^0+u_{k,l}) && \text{in } D-\Omega \\ \sigma_{ij}^0+\sigma_{ij} &= \overline{C}_{ijkl}(u_{k,l}^0+u_{k,l}) && \text{in } \Omega \end{aligned} \tag{21}$$

where C_{ijkl} and $\overline{C}_{ijkl}$ are the elastic moduli of the matrix and the inhomogeneity, respectively. The jump in the tangential displacement (slip) is denoted by $[u_i]=u_i(\text{out})-u_i(\text{in})$. $\sigma_{ij}^0 n_j$ and $\sigma_{ij}n_j$ are continuous on the interface of inhomogeneity $|\Omega|$. Then eqn (20) is expressed in terms of integrals in Ω or on $|\Omega|$ as

$$W^* = \frac{1}{2}\int_D \sigma_{ij}^0 u_{i,j}^0\,dV - \frac{1}{2}\int_\Omega \Delta C_{ijkl}(u_{k,l}^0+u_{k,l})u_{i,j}^0\,dV + \frac{1}{2}\int_{|\Omega|}\sigma_{ij}^0 n_j[u_i]\,dS \tag{22}$$

where $\Delta C_{ijkl}=\overline{C}_{ijkl}-C_{ijkl}$.

When the inhomogeneities are randomly distributed but $f \ll 1$, where f is the volume fraction ($f=\Omega/D$), the average elastic compliance $\tilde{S}_{ijkl}$ is obtained from eqn (22) as

$$\sigma_{ij}^0\varepsilon_{ij}^0 - \frac{f}{\Omega}\int_\Omega \Delta C_{ijkl}(u_{k,l}^0+u_{k,l})u_{i,j}^0\,dV + \frac{f}{\Omega}\int_{|\Omega|}\sigma_{ij}^0 n_j[u_i]\,dS = \langle\sigma_{ij}\rangle\langle\varepsilon_{ij}\rangle = \sigma_{ij}^0\langle\varepsilon_{ij}\rangle = \sigma_{ij}^0\tilde{S}_{ijkl}\sigma_{kl}^0 \tag{23}$$

where the average stress representation $\langle\sigma_{ij}\rangle=\sigma_{ij}^0$ is used.

When an isolated sliding inclusion Ω in domain D undergoes a constant eigenstrain, the elastic strain energy is expressed as

$$W^* = \frac{1}{2}\int_D \sigma_{ij}(u_{i,j}-\varepsilon_{ij}^*)\,dV \tag{24}$$

where the elastic strain is related to stress as

$$\begin{aligned} \sigma_{ij} &= C_{ijkl}(u_{k,l}-\varepsilon_{kl}^*) && \text{in } \Omega \\ \sigma_{ij} &= C_{ijkl}u_{k,l} && \text{in } D-\Omega. \end{aligned} \tag{25}$$

Note that

$$\int_D \sigma_{ij}u_{i,j}\,dV = -\int_{|\Omega|}\sigma_{ij}n_j[u_i]\,dS = 0. \tag{26}$$

We obtain this result by applying Gauss' theorem, where n_i is the outward unit vector normal to $|\Omega|$, and using the relations $\sigma_{ij,j}=0$ in D, $\sigma_{ij}n_j=0$ on $|D|$ and the fact that the product $\sigma_{ij}n_j[u_i]$ vanishes along the interface. Therefore eqn (24) becomes

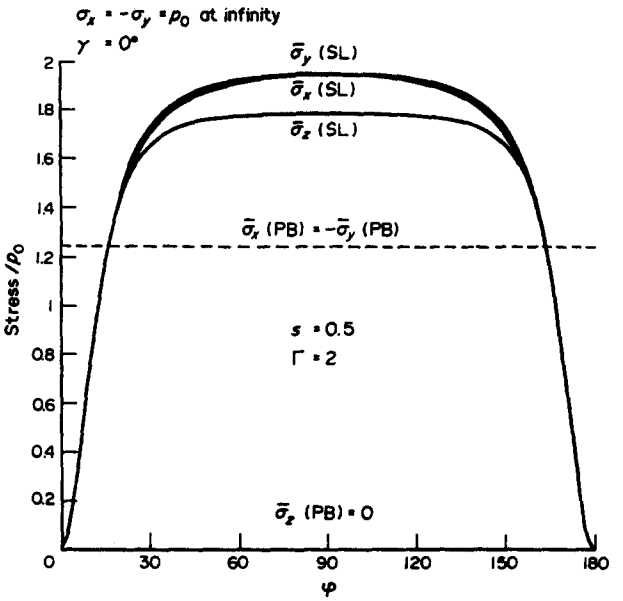

Fig. 2. Variation of $\bar{\sigma}_x$, $\bar{\sigma}_y$, $\bar{\sigma}_z$ in the inhomogeneity along the interface for sliding (SL) and perfect bonding (PB) when $s = a/b = 0.5$, $\nu = \bar{\nu} = 0.3$, $\Gamma = \bar{G}/G = 2$ and $\gamma = 0°$.

$$W^* = -\frac{1}{2}\varepsilon_{ij}^* \int_\Omega \sigma_{ij}\, dV. \tag{27}$$

For a random distribution of inclusions, the elastic strain energy per unit volume is

$$\frac{W^*}{D} = -\frac{1}{2}\varepsilon_{ij}^* \frac{f}{\Omega} \int_\Omega \sigma_{ij}\, dV. \tag{28}$$

DISCUSSION

The stress state at any point in the material depends on the elastic constants $\Gamma = \bar{G}/G$, ν, $\bar{\nu}$, the shape parameter $s = a/b$ (axis ratio or aspect ratio) and the position of the point. Γ is the ratio of the shear moduli and the limiting value $\Gamma = 0$ represents cavity and $\Gamma \to \infty$ corresponds to ideally rigid inhomogeneity. If $s = 1$, the subdomain is spherical in shape, $s \to \infty$ implies disk or penny shape in x–y plane, while $s \to 0$ can be interpreted as the needle-like shape or the infinite cylinder of radius a with the z-axis being its axis of symmetry. In the numerical results we take $\nu = \bar{\nu} = 0.3$ unless the effect of Poisson's ratio is investigated. The results for the sliding case denoted by (SL) are compared with the perfect bonding case (PB).

The essential difference between the solution representation for these two cases is that the sliding inclusion solution requires infinite series, and, if the same method is used, the finite series with $N = 4$ will give the exact solution for the perfect bonding case. For the sliding case, the infinite system of algebraic equations for A_n, B_n, C_n, $\bar{A}_n$, $\bar{B}_n$ and $\bar{C}_n$ is truncated to $N = 8$–30, where higher N is needed for s approaching the limiting case of the cylinder or disk shape. The sphere case $s = 1$ requires only a finite series representation.

The main difference in the results for sliding and perfect bonding cases is that stresses are not uniform in the inclusion when sliding takes place, unlike in the perfectly bonded inclusion as shown in Figs 2 and 3. The distribution of stresses $\bar{\sigma}_x$, $\bar{\sigma}_y$ and $\bar{\sigma}_z$ on the interface of the inhomogeneity is represented in Fig. 2 for SL and PB. The stresses are not uniform for the sliding case and they are all tensile for $\gamma = 0°$ (Fig. 2), almost zero for $\gamma = 45°$ and all compressive for $\gamma = 90°$, while for perfect bonding $\bar{\sigma}_x = -\bar{\sigma}_y$ and $\bar{\sigma}_z = 0$ everywhere in the inclusion. Figure 3 shows the variation of σ_x, σ_y in the inhomogeneity and in the matrix along the z-axis for both cases. Note that when sliding takes place, the stresses increase locally inside the inhomogeneity and in the matrix near the interface. Overall, however, there is a stress relaxation due to sliding which can be observed from the elastic strain energy calculations.

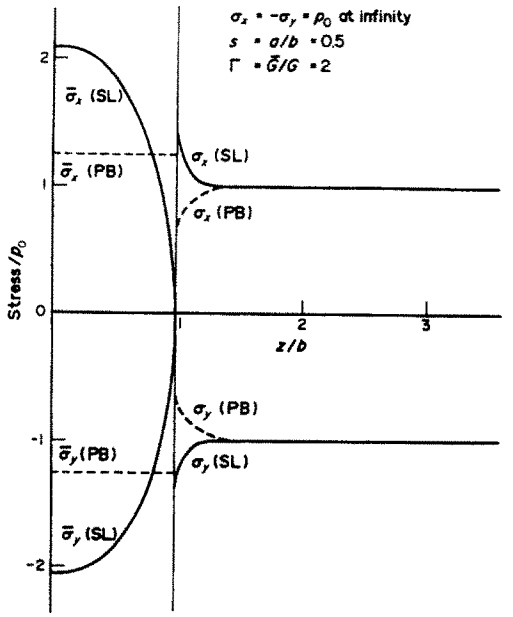

Fig. 3. Variation of σ_x, σ_y in the inhomogeneity and in the matrix along the z-axis for SL and PB.

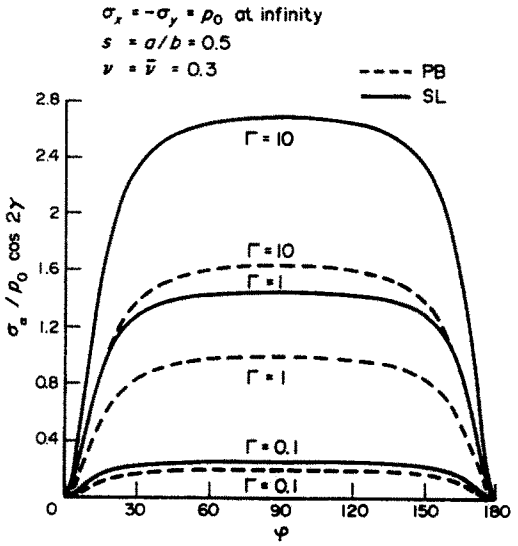

Fig. 4. Distribution of normal stress σ_α along the interface for various Γ for SL and PB.

The comparison of distribution of normal stress σ_α on the interface along φ for various shear moduli ratios Γ is shown in Fig. 4. The values on the graph need to be multiplied by $p_0 \cos 2\gamma$ to represent stress at any point on the interface. Angle φ is related to β by $\tan \varphi = (a/b) \tan \beta$. It is seen that the magnitude of σ_α increases with Γ and is much higher for the sliding case because of the shear stress relaxation. The effect of shape on the normal stress is presented in Fig. 5 and σ_α is highest in the x–y plane ($\varphi = 90°$) and when the sliding inclusion approaches a disk shape. These higher normal stresses due to the imperfect bond imply a higher tendency for debonding, void nucleation or crack initiation and propagation.

The stress concentration σ_x at $\varphi = 0°$ or 180° for $\Gamma = 0.1$, 0.5, 1, 2, 10 and shape parameter $0.25 \leqslant s < 4.0$ is compared with PB in Fig. 6. Observe that the magnitude of stresses for SL differs significantly from the PB case when Γ is large ("hard" inhomogeneity) and the effect of shape is more pronounced for $s < 1$. The highest stress at this point is for $s \to 0$ and $\Gamma \to 0$, which represents void of rod-like shape.

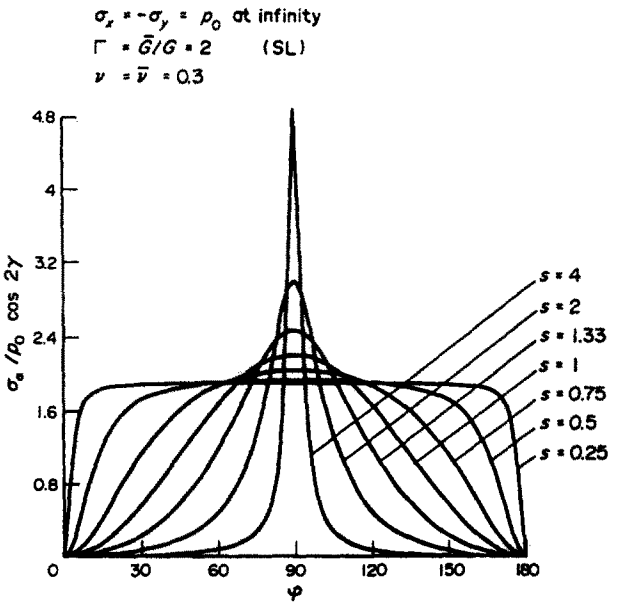

Fig. 5. Distribution of σ_α vs φ for various shape ratios for SL.

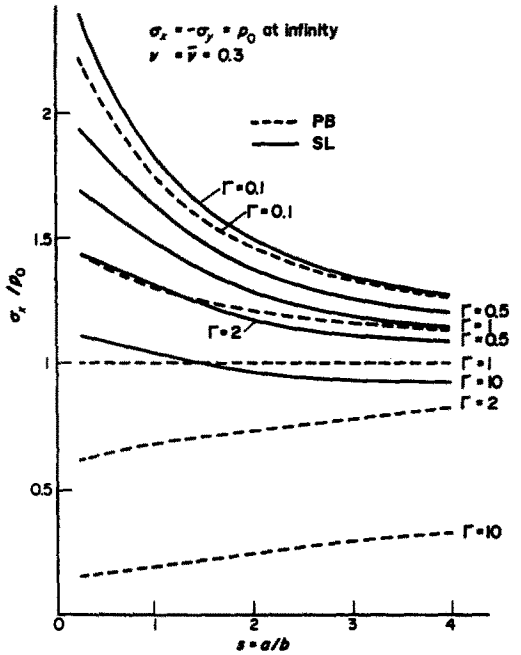

Fig. 6. σ_x in the matrix at polar point B as a function of shape ratio and Γ for SL and PB.

The behavior of slip quantity $2G\,[u_\beta]$ on the interface is shown in Figs 7 and 8. In Fig. 7 the sliding behavior for various Γ is shown for the case of shear load at infinity and it is observed that relative displacement $2G\,[u_\beta]$ is higher for the soft inhomogeneity. Figure 8 shows how $2G\,[u_\beta]$ changes with different inclusion shapes due to eigenstrains $\varepsilon_x^* = -\varepsilon_y^*$ in the inclusion. For the "long" shape most sliding takes place at ends ($\varphi = 0°$ or 180°) and for the "flat" shape around $\varphi = 90°$.

The stress $\bar{\sigma}_\beta$ in the inclusion for the eigenstrain case is shown in Figs 9(a) and (b) for SL and PB. It is interesting to observe that the curves are opposite in behavior, extremum values being at $\varphi = 90°$ for the sliding case and at $\varphi = 0°$ or 180° for the perfect bonding case.

The effect of Poisson's ratio is shown on the example of σ_γ in the matrix along the interface in Fig. 10. The interesting difference between sliding and perfect bonding is that for a perfectly bonded spheroid subjected to shear loading, elastic fields are independent of

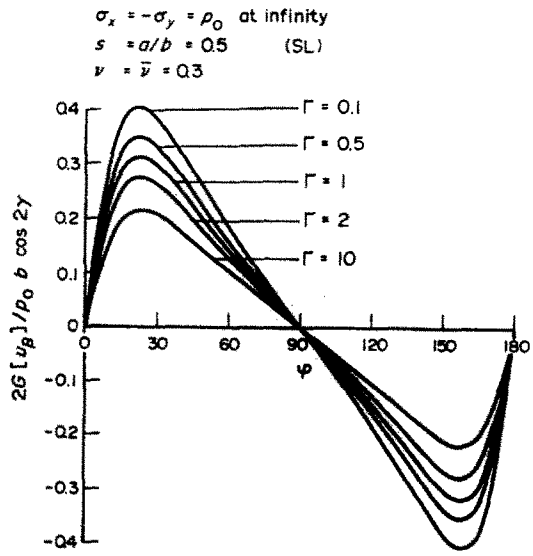

Fig. 7. Distribution of relative tangential displacement $2G\,[u_\beta]$ along φ for various Γ.

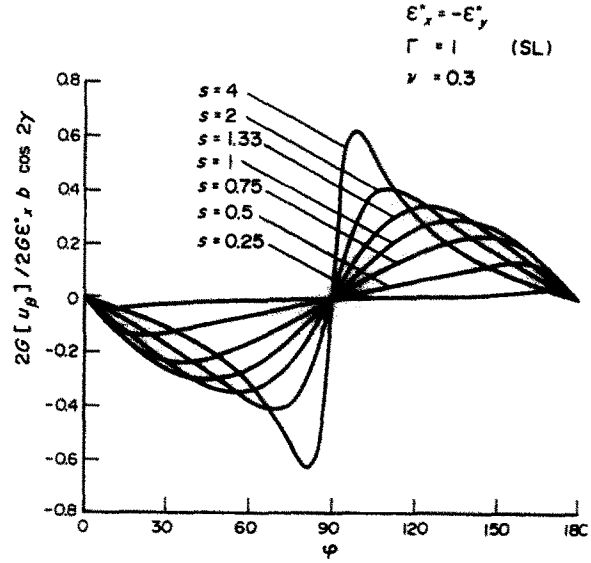

Fig. 8. Distribution of "slip" $2G\,[u_\beta]$ along φ for various shape ratios.

Poisson's ratio $\bar{\nu}$ of the inhomogeneity (see Edwards[2]), while the sliding inclusion solution depends on all parameters. However, the dependence on Poisson's ratios ν and $\bar{\nu}$ is small in comparison with that of Γ and s.

The shear solution presented in this paper, combined with the axisymmetric solution[6], yields to the solution for the uniaxial loading $\sigma^0_x = p_0$ at infinity or the eigenstrain $\varepsilon^*_x \neq 0$.

It might be noted that this solution for the special case of the sphere ($s = 1$) subjected to uniaxial loading at infinity agrees with Ghahremani's result[3] and the limit case when $\Gamma \to 0$ coincides with Sadowsky and Sternberg's[9] solution for the cavity.

When the composite with sliding inhomogeneities, representing fibers, for example, is subjected to shear loading at infinity, the ratio of the average shear modulus $\bar{\mu}$ of the composite and the shear modulus $G = \mu$ of the matrix is shown in Fig. 11 for various Γ and volume fraction f for both SL and PB when $s = 0.5$ and $\nu = \bar{\nu} = 0.3$. Sliding at the interfaces causes relaxation of the elastic moduli and the relaxation percentage is higher for large Γ or "hard" inhomogeneity. The "hardness" of inhomogeneities has a dominant effect on the macroscopic elastic moduli in comparison with the shape effect. Note that for the composites with sliding interfaces there is a Γ limit at which the average shear modulus

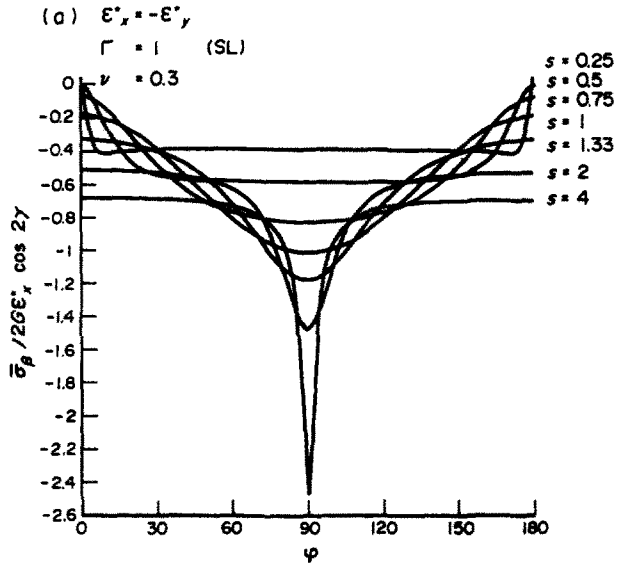

Fig. 9(a). Distribution of $\bar{\sigma}_\beta$ in the inclusion along the interface for various shape ratios for SL.

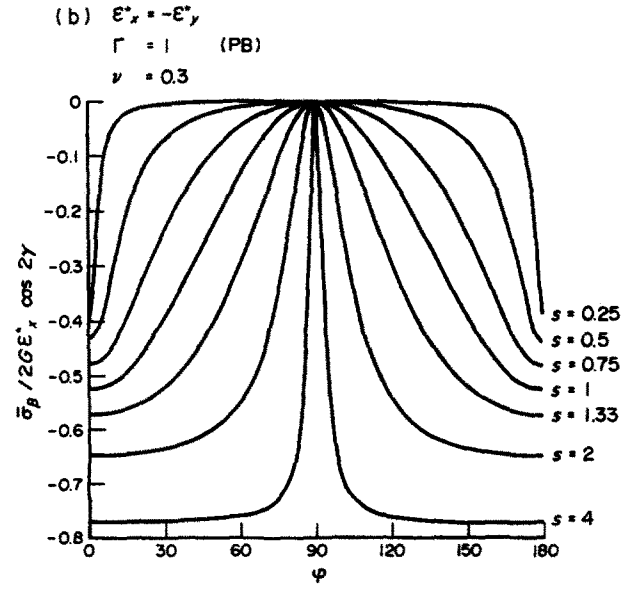

Fig. 9(b). Distribution of $\bar{\sigma}_\beta$ in the inclusion along φ for various shape ratios for PB.

starts decreasing even though the inhomogeneities have still higher shear modulus than the matrix.

The numerical comparison between the elastic strain energy of sliding and perfectly bonded inclusions undergoing constant shear eigenstrain for $\Gamma = 1.0$ and $\nu = \bar{\nu} = 0.3$ is shown in Table 1. Note that the elastic energy is much lower for the sliding inclusion, which implies the stress relaxation due to sliding.

CONCLUSION

The solution of the elastic fields due to a sliding spheroidal inclusion, which undergoes constant shear eigenstrains and a sliding inhomogeneity under uniform shear stress applied at infinity is presented.

The Papkovich–Neuber displacement potentials are used in the analysis. The sliding solution requires infinite series representation, while finite series give the exact solution for

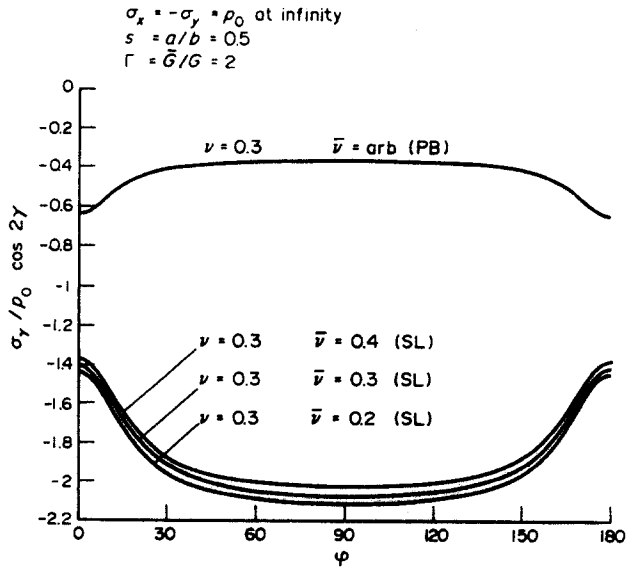

Fig. 10. The effect of Poisson's ratio $\bar{\nu}$ on σ_y in the matrix for constant $\nu = 0.3$ for SL and PB.

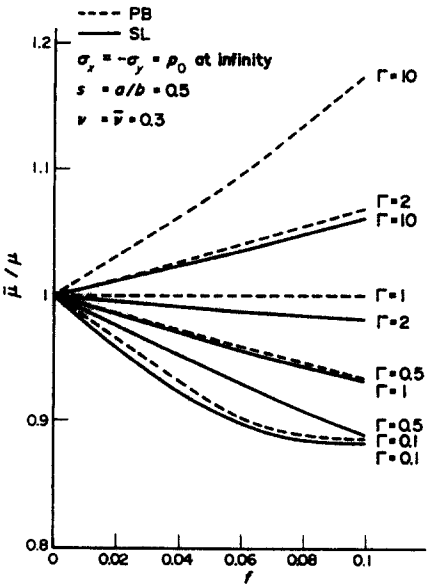

Fig. 11. Average shear moduli $\tilde{\mu}$ vs volume fraction f for various Γ for SL and PB.

Table 1. Comparison of elastic strain energy for sliding (SL) and perfectly bonded (PB) inclusion, when $\Gamma = 1$, $\nu = \bar{\nu} = 0.3$ and $\bar{W} = 2GW^*/[(2G\varepsilon_x^*)^2\Omega]$

s	$\bar{W}$ (PB)	$\bar{W}$ (SL)	Relaxation (%)
0.25	0.3879	0.2801	27.8
0.50	0.4353	0.2969	31.8
0.75	0.4818	0.3142	34.8
1.0	0.5240	0.3344	36.2
1.33	0.5720	0.3615	36.8
2.0	0.6462	0.4037	37.5
4.0	0.7698	0.4661	39.5

the perfect bonding case. When the sliding inclusion or inhomogeneity is of spherical shape, only finite series are required as shown by Ghahremani[3].

It is discovered that stresses in the sliding spheroidal subdomain are not uniform, unlike in the perfectly bonded inclusion where Eshelby's solution holds. The stress concentrations increase due to sliding (stresses are higher when the inhomogeneity is "soft" and of rod or cylinder shape).

The effect of interface is more pronounced when the shear modulus of the inhomogeneity is high in comparison with the shear modulus of the matrix. The ratio of the shear moduli and the shape of spheroid are significant factors affecting the stress concentrations, while the effect of Poisson's ratio is comparatively small.

The normal stress increases due to the imperfect bond (sliding), which implies higher tendency for debonding and cracking. The relative tangential displacement (slip) is higher for "soft" inhomogeneity.

Finally, sliding at the interfaces causes the relaxation of the average elastic moduli of the composite. This relaxation percentage is higher when the inhomogeneity is "hard" and the modular ratio has greater effect on the macroscopic properties than the shape.

Acknowledgment—The research was supported by the U.S. Army Grant No. DAAG29-85-k-0134.

REFERENCES

1. J. D. Eshelby, The determination of the elastic field of an ellipsoidal inclusion, and related problems. *Proc. R. Soc.* **A241**, 376–396 (1957).
2. R. H. Edwards, Stress concentration around spheroidal inclusions and cavities. *J. Appl. Mech.* **18**, 19–30 (1951).
3. F. Ghahremani, Effect of grain boundary sliding on anelasticity of polycrystals. *Int. J. Solids Structures* **16**, 825–845 (1980).
4. T. Mura and R. Furuhashi, The elastic inclusion with a sliding interface, *J. Appl. Mech.* **51**, 308–310 (1984).
5. G. T. Wong and D. M. Barnett, A dislocation method for solving 3-D crack and inclusion problems in linear elastic solids. In *Fundamentals of Deformation and Fracture* (Edited by B. A. Bilby, K. J. Miller and J. R. Willis), pp. 417–438. Cambridge University Press, Cambridge (1985).
6. T. Mura, I. Jasiuk and E. Tsuchida, The stress field of a sliding inclusion. *Int. J. Solids Structures* **21**, 1165–1179 (1985).
7. A. E. H. Love, *A Treatise on the Mathematical Theory of Elasticity*, 4th Edn. Dover, New York (1927).
8. E. W. Hobson, *The Theory of Spherical and Ellipsoidal Harmonics*. University Press, Cambridge (1931).
9. M. A. Sadowsky and E. Sternberg, Stress concentration around an ellipsoidal caviy in an infinite body under arbitrary plane stress perpendicular to the axis of revolution of cavity. *J. Appl. Mech.* **69**, A191–201 (1947).
10. E. Tsuchida and T. Mura, The stress field in an elastic half space having a spheroidal inhomogeneity under all-around tension parallel to the plane boundary. *J. Appl. Mech.* **50**, 807–816 (1983).